Synchronizing systolic calcium release with azumolene in an experimental model

Daoyuan Si, MD, PhD,*†[1] Praloy Chakraborty, MD,*[1] Mohammed Ali Azam, MBBS, PhD,* Madhav Krishna Kumar Nair,* Stéphane Massé, MASc,* Patrick F.H. Lai, MSc,* Christopher Labos, MD CM, MSc,‡ Sheila Riazi, MSc, MD,§ Kumaraswamy Nanthakumar, MD, FHRS*

*From the *The Hull Family Cardiac Fibrillation Management Laboratory, Toronto General Hospital, University Health Network, Toronto, Canada, †Department of Cardiology, China-Japan Union Hospital, Jilin University, Changchun, China, ‡Queen Elizabeth Health Complex, McGill University, Montréal, Canada, and §Malignant Hyperthermia Investigation Unit, Department of Anesthesia and Pain Management, University Health Network, Toronto, Canada.*

BACKGROUND Post-defibrillation myocardial contractile dysfunction adversely affects the survival of patients after cardiac arrest. Attenuation of diastolic calcium (Ca^{2+}) overload by stabilization of the cardiac ryanodine receptor (RyR2) is found to reduce refibrillation after long-duration ventricular fibrillation (LDVF).

OBJECTIVE In the present study, we explored the effects of RyR2 stabilization by azumolene on systolic Ca^{2+} release synchrony and myocardial contractility.

METHODS After completion of baseline optical mapping, Langendorff-perfused rabbit hearts were subjected to global ischemia followed by reperfusion with azumolene or deionized distilled water (vehicle). Following reperfusion, LDVF was induced with burst pacing. In the first series of experiments (n = 16), epicardial Ca^{2+} transient was analyzed for Ca^{2+} transient amplitude alternans and dispersion of Ca^{2+} transient amplitude alternans index (CAAI). In the second series of experiments following the same protocol (n = 12), ventricular contractility was assessed by measuring the left ventricular pressure.

RESULTS Ischemic LDVF led to greater CAAI (0.06 ± 0.02 at baseline vs 0.12 ± 0.02 post-LDVF, $P < .01$) and magnitude of dispersion of CAAI (0.04 ± 0.01 vs 0.09 ± 0.01, $P < .01$) in control hearts. In azumolene-treated hearts, no significant changes in CAAI (0.05 ± 0.01 vs 0.05 ± 0.01, $P = .84$) and dispersion of CAAI (0.04 ± 0.01 vs 0.04 ± 0.01, $P = .99$) were noted following ischemic LDVF. Ischemic LDVF was associated with reduction in left ventricular developed pressure (100% vs 36.8% ± 6.1%, $P = .002$) and dP/dt_{max} (100% vs 45.3% ± 6.5%, $P = .003$) in control hearts, but these reductions were mitigated (left ventricular developed pressure: 100% vs 74.0% ± 8.1%, $P = .052$, dP/dt_{max}: 100% vs 80.8% ± 7.9%, $P = .09$) in azumolene-treated hearts.

CONCLUSION Treatment with azumolene is associated with improvement of systolic Ca^{2+} release synchrony and myocardial contractility following ischemic LDVF.

KEYWORDS Azumolene; LDVF; Postresuscitation myocardial stunning; Ryanodine receptor; Ca^{2+} release synchrony

(Heart Rhythm O^2 2022;3:568–576)

Introduction

Mortality in patients with cardiovascular disease is significantly contributed by sudden cardiac death from ventricular fibrillation (VF).[1] Despite significant improvement in cardiopulmonary resuscitation (CPR) techniques and availability of timely and aggressive CPR, survival from cardiac arrest, particularly after prolonged CPR, is low.[2] Hemodynamic compromise from postresuscitation contractile dysfunction contributes significantly to early mortality following successful CPR.[3] Both duration and recurrence of VF are found to predict postresuscitation cardiac dysfunction.[4] Strategy to prevent VF recurrence by conventional ion channel modulators is complicated by hemodynamic instability owing to adverse effects from these drugs on cardiac and vascular contractility.[5,6] On the other hand, the use of clinically available inotropes may be associated with exacerbation of myocardial ischemia, arrhythmia, and mechanical dysfunction.[7]

Effective and synchronized systolic rise of intracellular Ca^{2+} ($[Ca^{2+}]_i$) by Ca^{2+}-induced Ca^{2+} release (CICR) is essential for the effective contraction of the heart.[8] During CICR, the Ca^{2+} release from individual ryanodine receptors (RyR2) at subcellular compartments contributes to the

[1]The first 2 authors contributed equally as first authors. **Address reprint requests and correspondence**: Dr Kumaraswamy Nanthakumar, Division of Cardiology, University Health Network, Toronto General Hospital, 150 Gerrard St West, GW3-526, Toronto, Ontario, Canada, M5G 2C4. E-mail address: kumar.nanthakumar@uhn.ca.

2666-5018/

https://doi.org/10.1016/j.hroo.2022.06.001

KEY FINDINGS

- Dispersion of calcium transient amplitude alternans may be used to measure spatial and temporal systolic Ca^{2+} release synchrony in the whole heart model.
- Dyssynchronous Ca^{2+} release in ischemic long-duration ventricular fibrillation (LDVF) is associated with reduced myocardial contractility.
- Restoration of Ca^{2+} release synchrony by the RyR2 stabilizer azumolene is associated with improvement of contractile function following ischemic LDVF.

generation of the Ca^{2+} sparks. Ca^{2+} transient at the cellular level represents the spatial and temporal summation of Ca^{2+} sparks.[9] Spatial and temporal dispersion of subcellular Ca^{2+} sparks is reported in various ischemic and nonischemic remodeling and has been linked to abnormal Ca^{2+} transient and contractile dysfunction in those conditions.[8,10–13] Despite an established link between dyssynchronous Ca^{2+} release and cardiac dysfunction, the pharmacological approach of treating cardiac contractile dysfunction by targeting systolic Ca^{2+} release synchrony has not been studied.

In our previous report, dantrolene sodium, originally described as a RyR stabilizer in skeletal muscle, facilitated successful defibrillation, and improved hemodynamic recovery from postischemic and post-defibrillation dysfunction.[14] Azumolene, a more water-soluble analog of dantrolene, was also found to reduce ventricular refibrillation and improve Ca^{2+} dynamics in a model of long-duration ventricular fibrillation (LDVF).[15] The current study was planned to evaluate the role of RyR2 modulation by azumolene on spatiotemporal systolic Ca^{2+} release synchrony and myocardial contractility in a model of ischemic LDVF. We hypothesize that spatiotemporal dyssynchrony in systolic Ca^{2+} release after ischemic LDVF is associated with reduction of cardiac contractility and that treatment with azumolene will lead to synchronized systolic Ca^{2+} release and mitigation of cardiac contractile dysfunction in this model.

Methods

All protocols followed the rules and regulations of the Canadian Council of Animal Care and were approved by the Animal Care Committee of the University Health Network.

Langendorff-perfused rabbit hearts

Explanted hearts from normal, healthy New Zealand White rabbits (male; 3.0–3.5 kg; Charles River Canada, Inc, Sherbrooke, Quebec, Canada) were used in these experiments. Following anesthesia with isoflurane, hearts were explanted through a midline thoracotomy. Each excised heart was then cannulated and mounted to a Langendorff setup, and perfused with a buffer solution consisting of (in mM) NaCl 130, $CaCl_2$ 2.2, KCl 4.4, $MgSO_4$ 0.3, $NaHCO_3$ 24, NaH_2PO_4 1.2, and glucose 12, and bubbled with 95% oxygen and 5% CO_2. The perfusion pressure of ~70 mm Hg and temperature of 37°C were maintained. Two silver electrodes on a plastic seat for the perfused heart were used for recording pseudo-surface electrocardiograph throughout the entire experimental period. An additional pair of electrodes were used for electrical stimulation/pacing.

Experimental protocol

After a brief period of stabilization, baseline Ca^{2+} optical mapping imaging measurements (n = 16) were obtained. In a separate series of experiments, left ventricular pressure (LVP) was measured (n = 12). The hearts were then subjected to perfusion arrest for 15 minutes to induce global ischemia. Following global ischemia, azumolene (20 μM; Toronto Research Chemicals, Inc, North York, Ontario, Canada) or the same volume of deionized distilled water alone (controls) was randomly chosen to be infused into the perfusate during reperfusion. After reperfusion, LDVF was induced with continuous burst pacing at 50 Hz at an output of +12 V for 6 minutes. After defibrillation with a 3 J shock, optical mapping measurement and LVP measurement were repeated (Figure 1).

Optical mapping

For optical mapping of the left ventricular (LV) epicardial fluorescence signals, Ca^{2+}-sensitive dye Rhod-2, AM (0.2 μmol; Biotium, Inc, Fremont, CA) was slowly infused into the perfusate solution. Blebbistatin (1 μmol; Enzo Life Sciences, Inc, Farmingdale, NY) was also added to the perfusate to eliminate motion artifacts during imaging. The fluorescence was excited with a xenon light source (Moritex, Saitama, Japan) and emission light was recorded with a high-speed CMOS camera (Ultima-L; Scimedia, Costa Mesa, CA). The 1-cm^2 sensor had 10,000 pixels organized in a 100 × 100 matrix, and imaging was performed at 500 frames/second using a THT splitter from Scimedia. The splitter was equipped with a Leica Planapo 0.63× lens on the objective side and a 1.0× lens on the condensing side. This provided a spatial resolution of 160 μm/pixel. Optical mapping was performed using the "pace and pause" protocol.[15]

Calcium dynamic parameter

After optical mapping, Ca^{2+} data were imported into MATLAB for signal processing and the following Ca^{2+} transient (CaT) parameters were calculated:

CaT amplitude alternans ratio

The beat-to-beat variation in amplitude of Ca^{2+} signals was defined as CaT amplitude alternans (CAA).[14] This was calculated as a ratio (smallest Ca^{2+} signals amplitude / largest Ca^{2+} signals amplitude), where the largest and smallest Ca^{2+} signals are each derived from either odd or even beats.[15]

Spatiotemporal heterogeneity of calcium handling

The magnitude of CAA was expressed as CaT amplitude alternans index (CAAI), 1 − X/Y, where X represents the average amplitude of the smaller Ca^{2+} transients and the

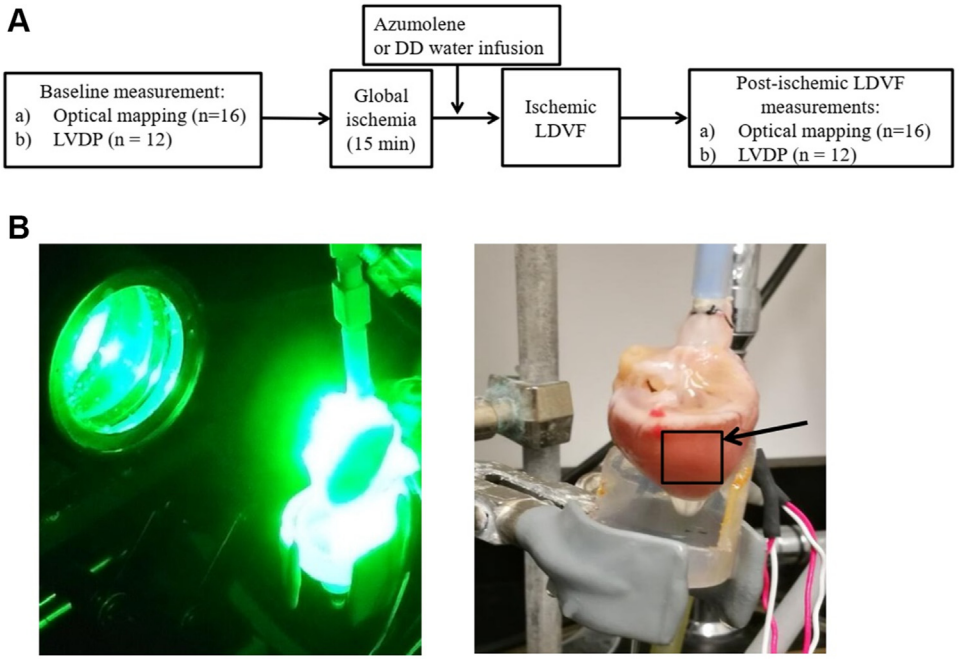

Figure 1 The experimental protocol and setup. **A:** The experimental protocol. **B:** The experimental setup and the heart during optical mapping (black square indicates approximately the area that was analyzed). DD water = deionized distilled water; LVDP = left ventricular developed pressure.

average amplitude of larger transients is represented by Y.[16] The mapping area (1.6 cm × 1.6 cm) on the LV anterior was divided into 100 × 100 points and CAAI was calculated in each of the 10,000 points' beats following a pace-and-pause protocol. The mean of CAAI was taken as a measure of global CAA and the dispersion of CAAI was used to calculate the spatiotemporal heterogeneity of Ca^{2+} handling. Alternans maps that represented the value of CAAI at each of 100 × 100 points were used to demonstrate the dispersion of CAAI. The CAAI values were shown in various colors, with red indicating lower CAAI and blue indicating higher values. Percentage of mapping area with nonsignificant alternans (the number of points with CAAI below 0.1 was expressed as a percentage of the total number of points, 10,000) and standard deviation of the distribution of CAAI in the spatial domain (10,000 points) were used to quantify the spatial heterogeneity of Ca^{2+} transient. As demonstrated previously in isolated rabbit hearts, optical imaging data recorded during pacing at 5 Hz were used for mapping and calculating the standard deviation (SD) of CAAI values.[17]

Left ventricular developed pressure measurement

In a separate set of Langendorff experiments, LV contractile function was determined by measuring the LVP with a balloon inserted in the chamber. The balloon was connected to the CyQ pressure transducer (CyberSense Inc, Nicholasville, KY) and our custom-made data acquisition system. At the beginning of the experiment, the LV end-diastolic pressure (LVEDP) was adjusted to approximately 10 mm Hg. The LVEDP, LV end-systolic pressure (LVESP), and dP/dt_{max} were continuously recorded following the above protocol. The detailed methodology for the measurement is described in our previous study.[18] The left ventricular developed pressure (LVDP) was calculated as LVESP − LVEDP. The data were collected and analyzed using LabChart Pro (ADInstruments Inc, Colorado Springs, CO).

Statistical analysis

Data are presented as the mean ± standard error (SE). Two-way analysis of variance with replication was performed to compare continuous variables (such as the calcium alternans [CA] index, SD of the CA index, LVDP, and dP/dt_{max}) at different time points between groups. A paired *t* test was used to compare baseline and post-LDVF variables in the same group. $P < .05$ was considered statistically significant. SPSS 17.0 (IBM, Armonk, NY) and GraphPad Prism 7.0 (GraphPad Software, San Diego, CA) were used for the data analysis.

Results

Effects of azumolene on global calcium transient

The heart rates were comparable between groups (control vs azumolene) at baseline (161.50 ± 2.16 vs 160.83 ± 1.92 beats per minute [bpm], $P = .79$), as well as after ischemic LDVF (128.50 ± 1.23 vs 127.83 ± 2.44 bpm, $P = .63$). Baseline global CAAI values were similar in both groups ($P = .88$); however, the CAAI in the control group demonstrated a significant increase in CAAI following ischemic LDVF (0.06 ± 0.02 at baseline to 0.12 ± 0.02 after VF, $P < .01$) (Figure 2). No significant change was noted in CAAI value after the ischemic LDVF in the azumolene-treated group (0.05 ± 0.01 at baseline and 0.05 ± 0.01 post-VF, $P = .84$) (Figure 2). CAA after LDVF was significantly less in azumolene-treated hearts than in the control group ($P = .01$; Figure 2B).

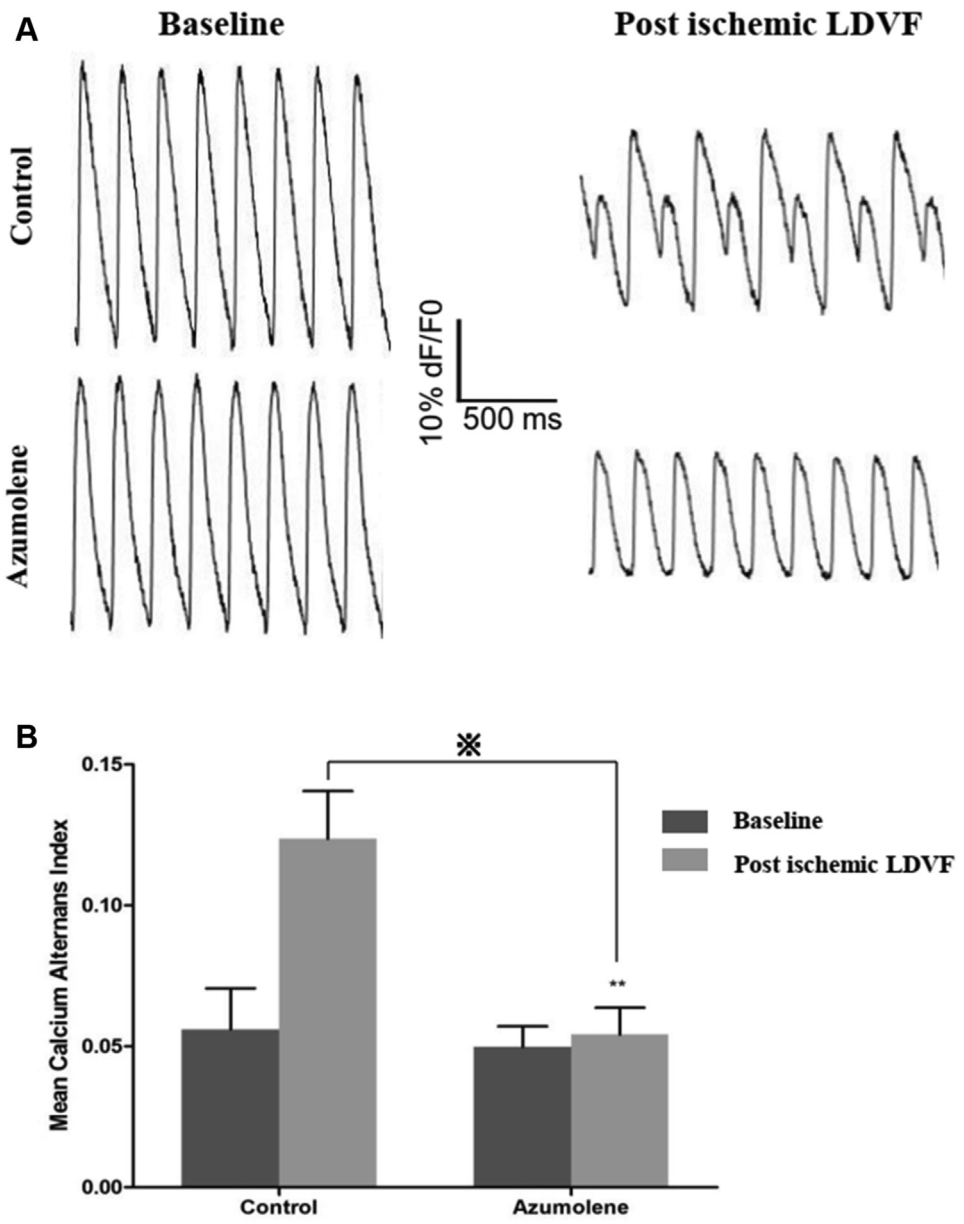

Figure 2 Effects of azumolene on temporal heterogeneity of calcium alternans. **A:** Calcium transients at baseline and after ischemic long-duration ventricular fibrillation (LDVF) in control and azumolene-treated hearts. **B:** Calcium alternans (CA) index at 5 Hz at baseline and after ischemic LDVF in the azumolene-treated group and control group (n = 8 in each group). In the control hearts, the CA index following ischemic LDVF was significantly increased from baseline (0.06 ± 0.02 vs 0.12 ± 0.02, $P < .01$). In the azumolene-treated hearts, azumolene significantly mitigated the increase in CA index (0.05 ± 0.01 at baseline and 0.05 ± 0.01 post-LDVF, $P = .84$). Furthermore, the CA index post-LDVF in the azumolene-treated hearts was significantly lower than that of the control hearts (0.05 ± 0.01 vs 0.12 ± 0.02, $P = .01$).

Effects of azumolene on CAAI dispersion

Figure 3A shows the dispersion of CAA in a colorimetric 2-dimensional map format with red indicating a lower CAAI and blue indicating a higher index, as shown in the color scale bar on the right of the figure. At baseline, CAAI across the epicardial surface were uniformly low in both groups, yielding CAAI maps that mainly displayed red pixels with little heterogeneity. Following ischemic LDVF, the CAAI were higher and they varied across the heart surface, leading to CAAI maps with a greater variety in colors, which included some blue pixels. To quantify the spatial heterogeneity of the CAAI in these rabbit hearts, we computed the number of points with a CAAI below 0.1 (an arbitrary threshold below which the CAA index is considered low). At baseline, CAAI are generally low (no or little alternans) across the heart (Figure 3A, left panels); the proportions of points with CAAI below 0.1 were 86.6% ± 4.8% and 89.8% ± 4.4% in the maps from the control and azumolene treatment arms, respectively (Figure 3B). For hearts in the control arm, the proportion

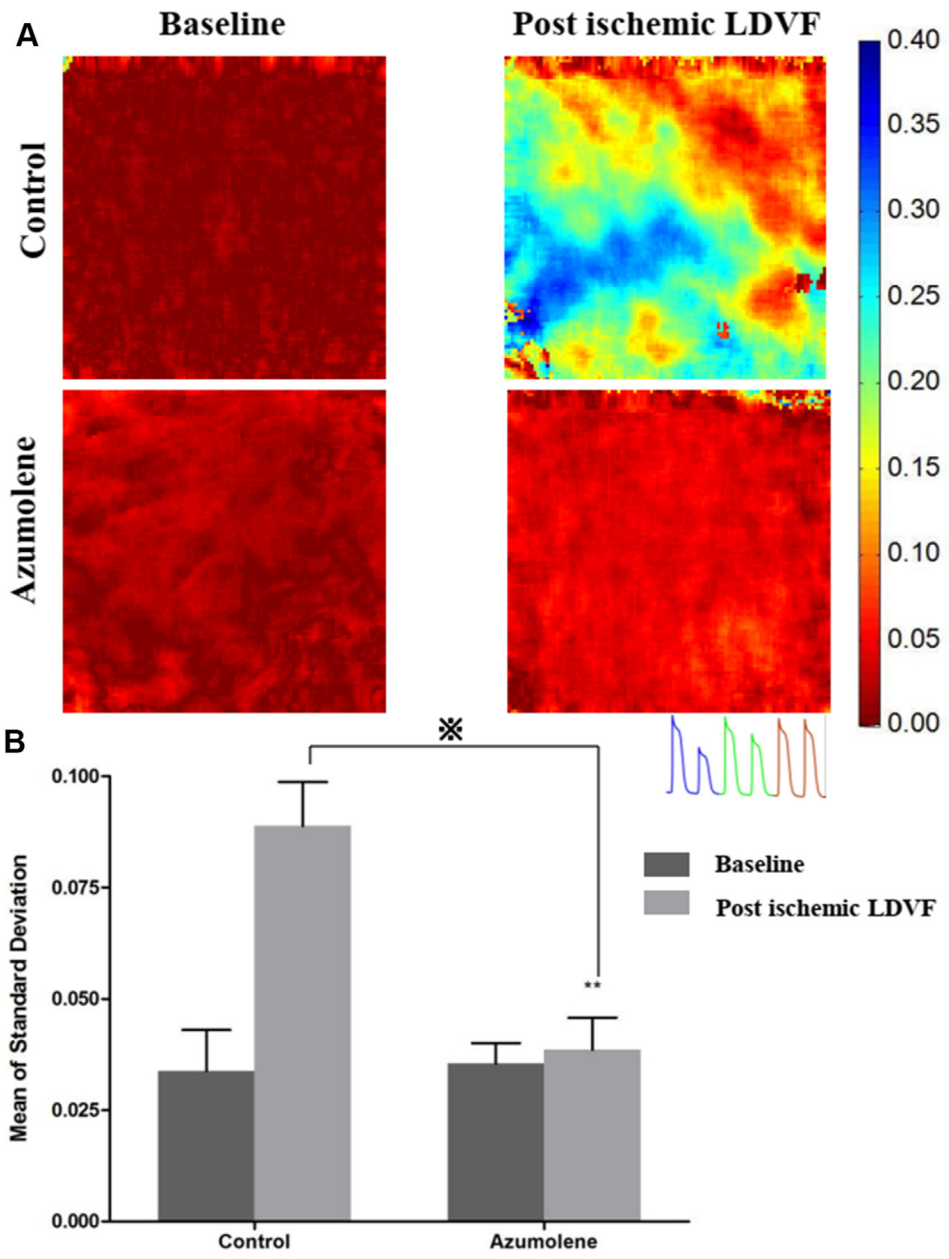

Figure 3 Effects of azumolene on spatial heterogeneity of calcium alternans. **A:** Color-coded alternans map showing the spatial dispersion of the CaT amplitude alternans index (CAAI) at baseline and after ischemic long-duration ventricular fibrillation (LDVF) in control and azumolene-treated hearts. **B:** Standard deviation (SD) of the spatial distribution of CAAI. CAAI at 5 Hz at baseline and after ischemic LDVF in the azumolene-treated group and nontreated control group (n = 8 in each group). In the alternans map, the values of CAAI at each of 100 × 100 points are shown in various colors, with red indicating lower CAAI and blue indicating higher values. A homogenous red color is indicative of reduced dispersion and low CAAI values, a marker of Ca^{2+} release synchrony. The heterogeneous color distribution indicates higher dispersion of CAAI and dyssynchronous Ca^{2+} release. In the control hearts, following ischemic LDVF, the SD of the CAAI was significantly increased from baseline (from 0.04 ± 0.01 to 0.09 ± 0.01, $P < .01$). Azumolene significantly mitigated the dispersion in the SD of the CAAI following ischemic LDVF (0.04 ± 0.01 vs 0.04 ± 0.01, $P = .99$).

of points with a low CAA index significantly decreased to 42.1% ± 5.8% after myopathic insult ($P = .03$). Heterogeneity in Ca^{2+} handling across the heart surface was not apparent in the azumolene-treated hearts, which continued to yield mostly red (low CAAI) maps after ischemic LDVF, with the proportion of points with a CAAI below 0.1 remaining high at 89.1% ± 4.3% ($P = .46$ vs baseline).

The variability in Ca^{2+} handling across the rabbit heart surface is also reflected in the SD of those CAAI used to generate the CAAI maps in Figure 3A. These mean SD values are shown in the graphs in Figure 3B. In the control hearts, the mean SD of CAAI across the maps increased significantly, from 0.04 ± 0.01 at baseline to 0.09 ± 0.01 after LDVF ($P < .01$, Figure 3B). In contrast, the mean values of the SD at baseline and after LDVF were not significantly

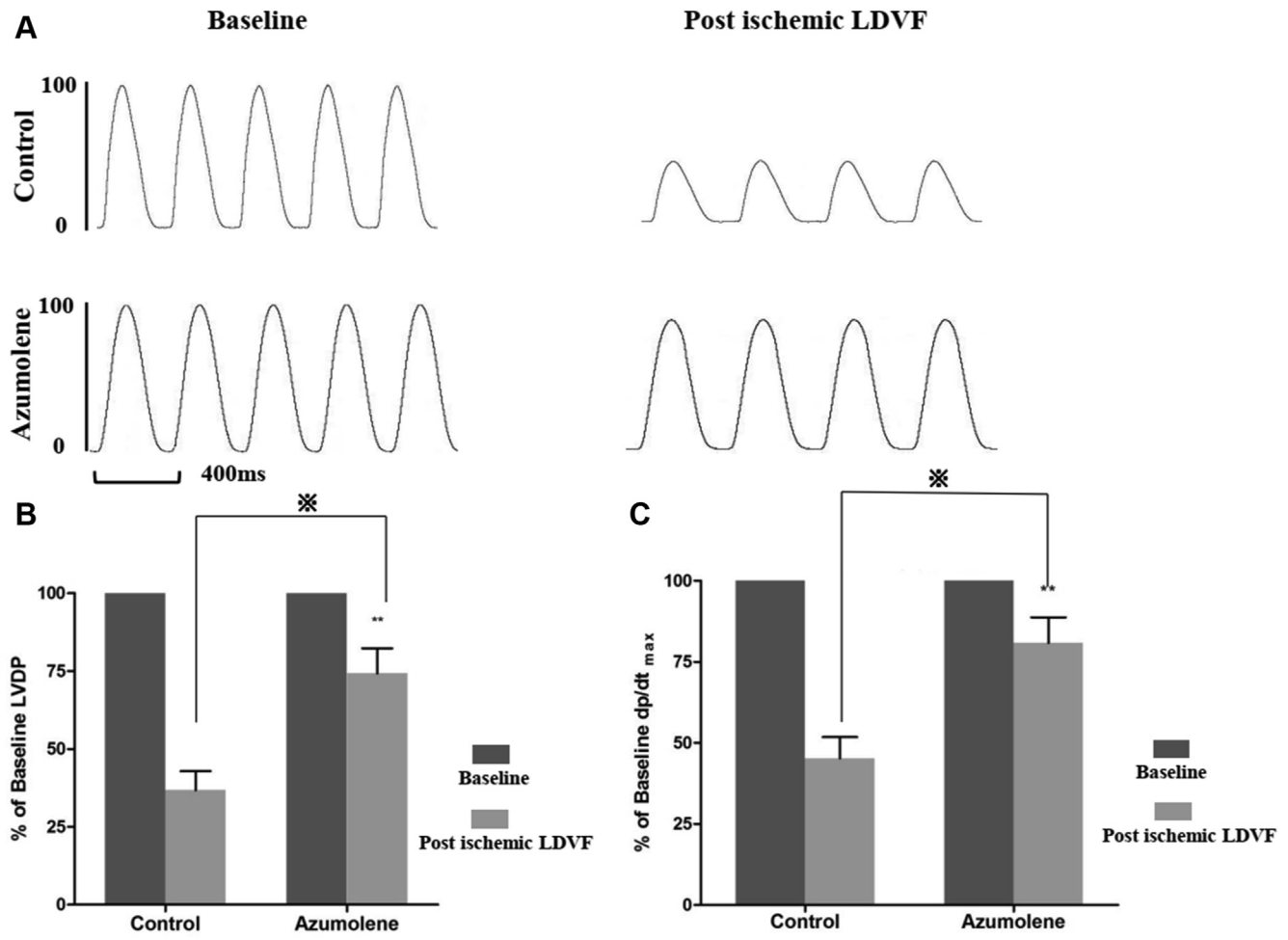

Figure 4 Effects of azumolene on contractility. **A:** Left ventricular developed pressure (LVDP) curves at baseline and after myopathic insult in the control and azumolene-treated hearts. **B:** LVDP at baseline and after ischemic long-duration ventricular fibrillation (LDVF) in the azumolene-treated and control hearts (n = 6 in each group). Azumolene significantly mitigated the decrease in LVDP following myocardial insult (74.0% ± 8.1% vs 36.8% ± 6.1% in control hearts, $P <$ .01). **C:** dP/dt_{max} at baseline and after myopathic insult in the azumolene-treated and untreated control hearts (n = 6 in each group). Azumolene significantly mitigated the decrease in dP/dt_{max} following ischemic LDVF (80.8% ± 7.9% vs 45.3% ± 6.5% in control hearts, P = .004).

different in the CAA index maps of the azumolene-treated hearts (0.04 ± 0.01 vs 0.04 ± 0.01, P = .99).

Effects of azumolene on cardiac contractility

In the second series of Langendorff experiments, there was no significant difference in heart rate between the 2 groups at baseline or after LDVF (data not shown). After LDVF, LVDP markedly decreased in the control hearts (Figure 4A). The LVDP and dP/dt_{max} were normalized to their respective baseline values and they were expressed as percentages of their baseline values. In the control hearts, LVDP significantly decreased after LDVF to 36.8% ± 6.1% of baseline (100% vs 36.8% ± 6.1%, P = .002; Figure 4B), while in the azumolene-treated hearts, the post-LDVF changes in LVDP, if any, were not statistically significant (100% vs 74.0% ± 8.1%, P = .052; Figure 4B). Similarly, dP/dt_{max} decreased in the control hearts to 45.3% ± 6.5% of baseline after myopathic insult (100% vs 45.3% ± 6.5%, P = .003; Figure 4C), while the change in dP/dt_{max} from baseline to after LDVF in the azumolene-treated hearts was not significant (100% vs 80.8% ± 7.9%, P = .09; Figure 4C). Following ischemic LDVF insult, LVDP (74.0% ± 8.1% vs 36.8% ± 6.1%, P = .003, Figure 4B) and dP/dt_{max} (80.8% ± 7.9% vs 45.3% ± 6.5%, P = .004, Figure 4C) were significantly higher in the azumolene-treated hearts, suggesting that the loss of contractility was mitigated by azumolene against LDVF-induced dysfunction.

Discussion

In the current study, we described a novel method for the assessment of spatial and temporal synchrony of Ca^{2+} release in the whole heart model. We also demonstrated that contractile dysfunction following long-duration VF is associated with heterogeneity in the systolic Ca^{2+} release mechanism and mitigation of Ca^{2+} release dyssynchrony with azumolene was associated with an attenuated loss of myocardial contraction in this model.

Assessment of spatial and temporal synchrony of Ca^{2+} release in whole heart model

Confocal microscopic imaging allowed the visualization of individual Ca^{2+} spark from each calcium release unit or couplon at the subcellular level.[19] Ca^{2+} transient at the whole-cell level is believed to result from coordinated spatial and temporal activation of multiple RyR2.[9,20] In previous reports, non-uniform subcellular Ca^{2+} release has been described in isolated cardiomyocytes from diverse pathophysiological conditions.[11–13,21–23] However, in the current study, we have described a novel method of assessing dispersion of Ca^{2+} release mechanisms based on beat-to-beat variability of CaT amplitude or Ca^{2+} transient alternans. Genesis of CaT amplitude alternans has been linked to spatial and temporal dyssynchrony in sarcoplasmic reticulum (SR) Ca^{2+} release owing to nonuniform activation and recovery of RyR2.[10,24] CAAI is indicative of the magnitude of Ca^{2+} transient amplitude alternans, ie, high CAAI indicates high variability. Optical Ca^{2+} imaging analysis by Qian and colleagues[17] reported significant spatial dispersion of CaT alternans on the epicardial surface of the ischemic rabbit ventricle. We propose that the epicardial distribution of CAAI is a marker of spatiotemporal dispersion of CaT at the whole heart level and the standard deviation of the distribution curve represents the magnitude of the dispersion. The current study demonstrated that the magnitude of spatial and temporal dispersion of Ca^{2+} was higher after ischemic LDVF, suggesting higher dyssynchrony with myocardial injury. Although the demonstration of Ca^{2+} release dyssynchrony in this model is a novel finding, reduced synchrony of Ca^{2+} release from RyR2 dysfunction has been demonstrated at the cellular level following acute or chronic myocardial stress.[8,10–13]

Systolic calcium release synchrony and azumolene

Preservation of sarcoplasmic Ca^{2+} release synchrony by azumolene following ischemic LDVF is another novel finding of our study. In our previous studies, we have reported the favorable effects of dantrolene and azumolene on cytosolic Ca^{2+} dynamics in models of VF.[14,15] Mitigation of diastolic Ca^{2+} elevation and Ca^{2+} alternans by azumolene was associated with reduction of VF recurrence in a model of ischemic LDVF.[15] Phosphorylation of Ser2808 of RyR2 by protein kinase A (PKA) was found to play a crucial role in the aberration of Ca^{2+} dynamics and the protective effect of azumolene was a consequence of stabilization of hyperphosphorylated RyR2. PKA-dependent hyperphosphorylation of Ser2808 of RyR2 is also reported in ischemia, heart failure, and diabetic cardiomyopathy.[13,23,25,26] PKA-mediated phosphorylation of RyR2 is associated with dissociation of RyR2 from FKBP12.6.[25] In the SR membrane, each subunit of RyR is closely associated with a subunit of FKBP12.6, an FK506-binding protein.[27] During CICR, FKBP12.6 plays a crucial role in the coordinated release of Ca^{2+} through coupled gating of arrays of RyR channels.[28,29] Dissociation of FKBP12.6 from phosphorylated RyR2 is reported to produce functional uncoupling of RyR2 channels, leading to random and stochastic activation of Ca^{2+} sparks.[25,28,30] Our previous study demonstrated that the cardioprotective effect of azumolene was due to the interaction of the agent with phosphorylated Ser2808-RyR2.[15] Binding FKBP12.6 with RyR2 is postulated to induce conformational changes and stabilize the channel.[31] In 3-dimensional structure analysis, both dantrolene and azumolene are reported to bind with RyR close to FK 506 binding site.[32] Stabilization of the interdomain interaction of hyperphorylated, destabilized RyR2 by azumolene may explain the restoration of coordinated Ca^{2+} release.[33]

Improvement of myocardial contractility by azumolene

Improvement of Ca^{2+} release synchrony in our experimental model was associated with improved myocardial contractility. Increased $[Ca^{2+}]_i$ during systole plays a crucial role in promoting actin-myosin interaction during myocardial contraction and abnormalities in Ca^{2+} transient are known to produce contractile dysfunction of the ventricle.[34,35] Inhomogeneities in Ca^{2+} release in the subcellular compartment are reported to produce a prolongation of systolic Ca^{2+} release time, defective excitation-contraction coupling, and reduced myocardial contractility.[11,13,36] Improvement in synchrony in Ca^{2+} release is found to improve myocardial contractility. Overexpression of FKBP12.6 in rabbit ventricular cardiomyocytes is associated with enhanced synchronicity of SR Ca^{2+} release and cell shortening.[37] Metabolic stabilization of RyR2 during normoxic perfusion in rodent cardiomyocytes is also found to be associated with shortening of systolic Ca^{2+} release and improved contractility.[38] Reduced myofilament Ca^{2+} sensitivity in face of normal CaT amplitude is previously described as a cause of post-defibrillation contractile dysfunction in the pacing-induced VF model.[39] However, the role of Ca^{2+} release synchrony in postresuscitation ventricular dysfunction has not been evaluated. In our study, contractile dysfunction after ischemic LDVF was associated with heterogeneities of SR Ca^{2+} release, and improved synchronicity by azumolene led to the improvement of myocardial contractility. Catecholamines are commonly used for hemodynamic support for postresuscitation cardiogenic shock syndrome. However, accentuation of CICR dyssynchrony[30] along with sinus tachycardia by adrenergic agonists may exacerbate the risk of arrhythmia and worsening of contractile dysfunction.[7] Antiarrhythmic efficacy of RyR2 stabilization is already reported.[14,15] The current finding may suggest a potential role of RyR stabilization as a new therapeutic strategy during cardiac resuscitation.

Limitations

Firstly, in this study, the role of azumolene on cytosolic Ca^{2+} release synchrony and myocardial contractility was evaluated but the effect on arrhythmia was not evaluated. However, the reduction of ventricular arrhythmia by RyR2

modulation has already been evaluated in our previous studies.[14,15] Second, the underlying molecular mechanisms of improved Ca^{2+} release synchrony are not explored in this study. We have previously described that the stabilization of phosphorylated RyR2 by azumolene is responsible for its favorable effects on Ca^{2+} dynamics.[15] We acknowledge the limitation of the denervated, isolated, perfused heart model. The results should be interpreted with caution, and evaluation of effects needs additional studies with in vivo characterization. Finally, estrogen is reported to modify the cytosolic Ca^{2+} dynamics[40]; to eliminate the confounding from temporal variation of female sex hormones, we have included only male rabbits in our study, and we acknowledge that the study findings carry the limitation of generalizability. The current study is hypothesis-generating; a future study including both male and female animals will provide more robust data.

Conclusion

In isolated heart preparations, ischemic LDVF was associated with enhanced spatial and temporal dispersion of systolic Ca^{2+} release and reduced myocardial contractility. Treatment with azumolene resulted in a reduction of Ca^{2+} release dyssynchrony. Azumolene treatment was also associated with improvement of LV contractile function after LDVF. Mitigation of Ca^{2+} release dyssynchrony and contractile dysfunction by azumolene may provide protection against postresuscitation left ventricular dysfunction.

Acknowledgments

K.N. is a recipient of the Mid-Career Investigator Award from the Heart & Stroke Foundation of Ontario. The authors are grateful to Mr Arulalan Veluppillai for his help in producing graphics in this manuscript.

Funding Sources: This research was supported by an operating grant from the Canadian Institutes of Health Research (MOP 142272).

Disclosures: K.N. is a consultant for Servier, Biosense Webster, Abbott, and BlueRock. S.M. is a consultant for Abbott. S.R. has received consulting fee from Norgine Pharmaceuticals.

Authorship: All authors attest they meet the current ICMJE criteria for authorship.

Ethics Statement: All protocols followed the rules and regulations of the Canadian Council of Animal Care and were approved by the Animal Care Committee of the University Health Network.

References

1. Go AS, Mozaffarian D, Roger VL, et al. Heart disease and stroke statistics–2013 update: a report from the American Heart Association. Circulation 2013;127:e6–e245.
2. Nadkarni VM, Larkin GL, Peberdy MA, et al. First documented rhythm and clinical outcome from in-hospital cardiac arrest among children and adults. JAMA 2006;295:50–57.
3. Neumar RW, Nolan JP, Adrie C, et al. Post–cardiac arrest syndrome. Circulation 2008;118:2452–2483.
4. Yao Y, Johnson NJ, Perman SM, Ramjee V, Grossestreuer AV, Gaieski DF. Myocardial dysfunction after out-of-hospital cardiac arrest: predictors and prognostic implications. Intern Emerg Med 2018;13:765–772.
5. American Heart Association (AHA). 2005 AHA guidelines for cardiopulmonary resuscitation and emergency cardiovascular care. Part 7.2: management of cardiac arrest. Circulation 2005;112(24 Supplement):IV-58–IV-66.
6. Sheu SS, Lederer WJ. Lidocaine's negative inotropic and antiarrhythmic actions. Dependence on shortening of action potential duration and reduction of intracellular sodium activity. Circ Res 1985;57:578–590.
7. Overgaard CB, Džavík V. Inotropes and vasopressors. Circulation 2008;118:1047–1056.
8. Heinzel FR, MacQuaide N, Biesmans L, Sipido K. Dyssynchrony of Ca^{2+} release from the sarcoplasmic reticulum as subcellular mechanism of cardiac contractile dysfunction. J Mol Cell Cardiol 2011;50:390–400.
9. Wier WG, Balke CW. Ca^{2+} release mechanisms, Ca^{2+} sparks, and local control of excitation-contraction coupling in normal heart muscle. Circ Res 1999;85:770–776.
10. Díaz ME, Eisner DA, O'Neill SC. Depressed ryanodine receptor activity increases variability and duration of the systolic Ca^{2+} transient in rat ventricular myocytes. Circ Res 2002;91:585–593.
11. Harris DM, Mills GD, Chen X, et al. Alterations in early action potential repolarization causes localized failure of sarcoplasmic reticulum Ca^{2+} release. Circ Res 2005;96:543–550.
12. Heinzel FR, Bito V, Biesmans L, et al. Remodeling of T-tubules and reduced synchrony of Ca^{2+} release in myocytes from chronically ischemic myocardium. Circ Res 2008;102:338–346.
13. Shao CH, Rozanski GJ, Patel KP, Bidasee KR. Dyssynchronous (non-uniform) Ca^{2+} release in myocytes from streptozotocin-induced diabetic rats. J Mol Cell Cardiol 2007;42:234–246.
14. Zamiri N, Massé S, Ramadeen A, et al. Dantrolene improves survival after ventricular fibrillation by mitigating impaired calcium handling in animal models. Circulation 2014;129:875–885.
15. Si D, Azam MA, Lai PFH, et al. Essential role of ryanodine receptor 2 phosphorylation in the effect of azumolene on ventricular arrhythmia vulnerability in a rabbit heart model. J Cardiovasc Electrophysiol 2018;29:1707–1715.
16. Wu Y, Clusin WT. Calcium transient alternans in blood-perfused ischemic hearts: observations with fluorescent indicator fura red. Am J Physiol 1997;273:H2161–H2169.
17. Qian YW, Clusin WT, Lin SF, Han J, Sung RJ. Spatial heterogeneity of calcium transient alternans during the early phase of myocardial ischemia in the blood-perfused rabbit heart. Circulation 2001;104:2082–2087.
18. Azam MA, Wagg CS, Massé S, et al. Feeding the fibrillating heart: dichloroacetate improves cardiac contractile dysfunction following VF. Am J Physiol Heart Circ Physiol 2015;309:H1543–H1553.
19. Cheng H, Lederer WJ, Cannell MB. Calcium sparks: elementary events underlying excitation-contraction coupling in heart muscle. Science 1993;262:740–744.
20. Bers Donald M, Fill M. Coordinated feet and the dance of ryanodine receptors. Science 1998;281:790–791.
21. Litwin SE, Zhang D, Bridge JHB. Dyssynchronous Ca^{2+} sparks in myocytes from infarcted hearts. Circ Res 2000;87:1040–1047.
22. Louch WE, Bito V, Heinzel FR, et al. Reduced synchrony of Ca^{2+} release with loss of T-tubules - a comparison to Ca^{2+} release in human failing cardiomyocytes. Cardiovasc Res 2004;62:63–73.
23. Yaras N, Ugur M, Ozdemir S, et al. Effects of diabetes on ryanodine receptor Ca release channel (RyR2) and Ca^{2+} homeostasis in rat heart. Diabetes 2005;54:3082–3088.
24. Weiss JN, Nivala M, Garfinkel A, Qu Z. Alternans and arrhythmias: from cell to heart. Circ Res 2011;108:98–112.
25. Marx SO, Reiken S, Hisamatsu Y, et al. PKA phosphorylation dissociates FKBP12.6 from the calcium release channel (ryanodine receptor): defective regulation in failing hearts. Cell 2000;101:365–376.
26. Wehrens XH, Lehnart SE, Reiken S, Vest JA, Wronska A, Marks AR. Ryanodine receptor/calcium release channel PKA phosphorylation: a critical mediator of heart failure progression. Proc Natl Acad Sci U S A 2006;103:511–518.
27. Brillantes A-MB, Ondrias K, Scott A, et al. Stabilization of calcium release channel (ryanodine receptor) function by FK506-binding protein. Cell 1994;77:513–523.
28. Marx SO, Gaburjakova J, Gaburjakova M, Henrikson C, Ondrias K, Marks AR. Coupled gating between cardiac calcium release channels (ryanodine receptors). Circ Res 2001;88:1151–1158.
29. Marx SO, Ondrias K, Marks AR. Coupled gating between individual skeletal muscle Ca^{2+} release channels (ryanodine receptors). Science 1998;281:818–821.
30. Zhao YT, Guo YB, Gu L, et al. Sensitized signalling between L-type Ca^{2+} channels and ryanodine receptors in the absence or inhibition of FKBP12.6 in cardiomyocytes. Cardiovasc Res 2017;113:332–342.
31. Sharma MR, Jeyakumar LH, Fleischer S, Wagenknecht T. Three-dimensional visualization of FKBP12.6 binding to an open conformation of cardiac ryanodine receptor. Biophys J 2006;90:164–172.
32. Wang R, Zhong X, Meng X, et al. Localization of the dantrolene-binding sequence near the FK506-binding protein-binding site in the three-

dimensional structure of the ryanodine receptor. J Biol Chem 2011; 286:12202–12212.
33. Murayama T, Oba T, Kobayashi S, Ikemoto N, Ogawa Y. Postulated role of interdomain interactions within the type 1 ryanodine receptor in the low gain of Ca^{2+}-induced Ca^{2+} release activity of mammalian skeletal muscle sarcoplasmic reticulum. Am J Physiol Cell Physiol 2005; 288:C1222–C1230.
34. Beuckelmann DJ, Näbauer M, Erdmann E. Intracellular calcium handling in isolated ventricular myocytes from patients with terminal heart failure. Circulation 1992;85:1046–1055.
35. Piacentino V, Weber CR, Chen X, et al. Cellular basis of abnormal calcium transients of failing human ventricular myocytes. Circ Res 2003;92:651–658.
36. Houser SR, Piacentino V 3rd, Weisser J. Abnormalities of calcium cycling in the hypertrophied and failing heart. J Mol Cell Cardiol 2000;32:1595–1607.
37. Gómez AM, Schuster I, Fauconnier J, Prestle J, Hasenfuss G, Richard S. FKBP12.6 overexpression decreases Ca^{2+} spark amplitude but enhances $[Ca^{2+}]_i$ transient in rat cardiac myocytes. Am J Physiol Heart Circ Physiol 2004;287:H1987–H1993.
38. Jaimes R 3rd, Kuzmiak-Glancy S, Brooks DM, Swift LM, Posnack NG, Kay MW. Functional response of the isolated, perfused normoxic heart to pyruvate dehydrogenase activation by dichloroacetate and pyruvate. Pflugers Arch 2016;468:131–142.
39. Zaugg CE, Ziegler A, Lee RJ, Barbosa V, Buser PT. Postresuscitation stunning: postfibrillatory myocardial dysfunction caused by reduced myofilament Ca^{2+} responsiveness after ventricular fibrillation-induced myocyte Ca^{2+} overload. J Cardiovasc Electrophysiol 2002;13:1017–1024.
40. Mahmoodzadeh S, Dworatzek E. The role of 17β-estradiol and estrogen receptors in regulation of Ca^{2+} channels and mitochondrial function in cardiomyocytes. Front Endocrinol (Lausanne) 2019;10:310.